Title

Epistatic Transcription Factor Networks Differentially Modulate Arabidopsis Growth and Defense

Journal

Genetics, 214(2)

ISSN

0016-6731

Authors

Li, Baohua
Tang, Michelle
Caseys, Céline
et al.

Publication Date

2020-02-01

DOI

10.1534/genetics.119.302996

Peer reviewed

Epistatic Transcription Factor Networks Differentially Modulate *Arabidopsis* Growth and Defense

Baohua Li,*,†,1 Michelle Tang,*,‡,1 Céline Caseys,*,1 Ayla Nelson,* Marium Zhou,* Xue Zhou,* Siobhan M. Brady,‡ and Daniel J. Kliebenstein*,§,2

*Department of Plant Sciences, University of California, Davis, California 95616, †College of Horticulture, Northwest A&F University, Yangling, Shaanxi, 712100, China, ‡Department of Plant Biology and Genome Center, University of California, Davis, California 95616, and §DynaMo Center of Excellence, University of Copenhagen, DK-1871 Frederiksberg C, Denmark

ORCID IDs: 0000-0001-7235-0470 (B.L.); 0000-0002-8779-8697 (M.T.); 0000-0003-4187-9018 (C.C.); 0000-0002-2586-0264 (X.Z.); 0000-0001-9424-8055 (S.M.B.); 0000-0001-5759-3175 (D.J.K.)

ABSTRACT Plants integrate internal and external signals to finely coordinate growth and defense for maximal fitness within a complex environment. A common model suggests that growth and defense show a trade-offs relationship driven by energy costs. However, recent studies suggest that the coordination of growth and defense likely involves more conditional and intricate connections than implied by the trade-off model. To explore how a transcription factor (TF) network may coordinate growth and defense, we used a high-throughput phenotyping approach to measure growth and flowering in a set of single and pairwise mutants previously linked to the aliphatic glucosinolate (GLS) defense pathway. Supporting a link between growth and defense, 17 of the 20 tested defense-associated TFs significantly influenced plant growth and/or flowering time. The TFs' effects were conditional upon the environment and age of the plant, and more critically varied across the growth and defense phenotypes for a given genotype. In support of the coordination model of growth and defense, the TF mutant's effects on short-chain aliphatic GLS and growth did not display a simple correlation. We propose that large TF networks integrate internal and external signals and separately modulate growth and the accumulation of the defensive aliphatic GLS.

KEYWORDS epistasis; glucosinolates; plant defense; plant growth; transcription factor

GROWTH and defense are essential biological processes necessary for plant survival. Optimizing fitness requires plants to coordinate growth and defense phenotypes in response to specific environments. Efforts to understand the relationship between plant growth and defense are often modeled as a trade-off where resistance and growth are a cost on each other (Karban and Baldwin 1997; Agrawal 2011a,b; Huot *et al.* 2014). This model assumes that the available resources for plants are limited, suggesting that any flux of resources, energy and elements into plant defense would be at the cost of plant growth. Support for this model comes from the observations that some constitutive defense mutants generally grow smaller and suffer from yield and/or fitness losses.

A developing model is emerging from research in ecology, evolutional biology, and molecular genetics that suggests a dynamic relationship between plant defense and growth (Singh *et al.* 2002; de Lucas *et al.* 2016). This model began with multiple reports showing that defense metabolism does not show a universal negative correlation with plant growth (Bergelson and Purrington 1996; Almeida-Cortez *et al.* 1999; Koricheva 2002). Additionally, mechanistic manipulations of defense metabolism can show little to no effect on plant growth. Further, diminutive constitutive defense mutants can have their growth rescued by second-site mutations that maintain the constitutive defense (Hemm *et al.* 2003; Paul-Victor *et al.* 2010; Züst *et al.* 2011; Joseph *et al.* 2013; Campos *et al.* 2016; Kliebenstein 2016). Finally, support for this model came from the identification of specific transcription factors (TFs) that simultaneously increase growth and

doi: https://doi.org/10.1534/genetics.119.302996
Manuscript received August 7, 2019; accepted for publication December 17, 2019; published Early Online December 18, 2019.
Supplemental material available at figshare: https://doi.org/10.25386/genetics.11388195.
[1]These authors contributed equally to this study.
[2]Corresponding author: University of California, Davis, One Shields Ave., Davis, CA 95616. E-mail: Kliebenstein@ucdavis.edu

defenses (Campos *et al.* 2016; Wang *et al.* 2018). Together, these observations suggest that the relationship between plant defense and growth is a complex and active internal decision process involving regulatory and signaling pathways *in planta* (Kliebenstein 2016; Züst and Agrawal 2017).

Several recent studies provide important insights about the roles TFs play in integrating and transducing internal and external signals essential to growth and defense (Singh *et al.* 2002; Pajerowska-Mukhtar *et al.* 2012; Lozano-Duran *et al.* 2013; Fan *et al.* 2014; de Lucas *et al.* 2016). Mutations in *JAZs* (transcriptional repressors in jasmonic acid signaling pathway) in combination with altered photoreceptor *PhyB* result in fast-growing plants with enhanced plant defense responses (Campos *et al.* 2016). In rice, the *Ideal Plant Architecture 1* TF activates yield-related genes while promoting both plant defense and rice yield (Jiao *et al.* 2010; Wang *et al.* 2018). These case studies demonstrate that growth and defense are under complex regulation and that TFs can be key integrators to coordinate these two important biological processes. However, it is not clear if these examples are isolated instances or a more generalizable view of how TFs modulate growth and defense. Systemic studies on TFs and their regulatory networks are needed to test how TFs may or may not coordinate between plant defense and growth in diverse environmental settings.

To explore the interplay between plant growth and defense, we used the well-characterized plant secondary metabolic pathway, the *Arabidopsis* methionine-derived aliphatic glucosinolate (GLS) (Sønderby *et al.* 2010b). Aliphatic GLS provide defense against numerous herbivorous insects in both the laboratory and the field (Lambrix *et al.* 2001; Schlaeppi *et al.* 2008; Kos *et al.* 2012; Beran *et al.* 2014; Falk *et al.* 2014; Kerwin *et al.* 2015, 2017; Zalucki *et al.* 2017). Aliphatic GLS are critical for fitness in Brassicales, and their specific composition and accumulation across developmental stages are intricately controlled by genetic variation and pleiotropically influence a variety of growth- and defense-related pathways (Kliebenstein *et al.* 2002a; Bidart-Bouzat and Kliebenstein 2008; Wentzell and Kliebenstein 2008; Burow *et al.* 2010; Kerwin *et al.* 2011; Züst *et al.* 2011). Since aliphatic GLS contain both sulfur and nitrogen, flux-based modeling suggests that they are expensive to produce as they can accumulate at high concentrations. However, mutants missing these compounds have at most a slight change in early growth, indicating that aliphatic GLS do not display a tight trade-off with growth (Paul-Victor *et al.* 2010; Züst *et al.* 2011; Bekaert *et al.* 2012). Instead, the regulatory complexity of the aliphatic GLS better fits with the coordination model. For example, a large-scale yeast one-hybrid study identified a large collection of TFs that bind the aliphatic GLS enzyme promoters and regulate aliphatic GLS accumulation, directly arguing against a single dominant TF model (Li *et al.* 2014). Further, these TFs showed extensive epistatic interactions in influencing the accumulation of GLS (Li *et al.* 2018). This suggests that the regulation of this defense pathway is highly complex. While aliphatic GLS levels are influenced by perception of jasmonic acid and other herbivory-related signals, the majority of their accumulation is a steady-state response to the environment with genetic variation between natural accessions having larger effects on accumulation than specific signal perception events (Kliebenstein *et al.* 2002b; Mikkelsen *et al.* 2003; Wentzell and Kliebenstein 2008; Chan *et al.* 2011; Guo *et al.* 2013; Pangesti *et al.* 2016). Thus, we focused on using genetic perturbation of aliphatic short-chain (SC) GLS accumulation, the major form of aliphatic GLS, as an optimal way to test the system and how epistasis may link defense, growth, and flowering.

To test the conditional model of growth and defense, we used high-throughput phenotyping to measure growth and flowering time of 20 single TF mutants and 48 double mutants previously shown to influence the *Arabidopsis* aliphatic GLS pathway in two environments (Sønderby *et al.* 2007; Li *et al.* 2018). We show that 17 of the 20 TFs significantly influence plant growth and/or plant flowering time. While most TFs influence growth and defense, there was no clear correlation between the aliphatic SC GLS accumulation and plant growth and flowering time in our study. This indicates that each TF has specific and independent influences on both growth and aliphatic GLS. Our findings support the coordination model for the relationship between plant growth and aliphatic GLS, and provide novel insights on how these critical and complex biological processes are integrated to optimize fitness in different environments.

Materials and Methods

Plant materials, growth conditions, and experimental design

The *Arabidopsis thaliana* transfer DNA (T-DNA) insertion lines of the 20 TFs were ordered from *Arabidopsis* Biological Resource Center (Sussman *et al.* 2000; Alonso *et al.* 2003) and homozygous lines were validated in previous studies (Sønderby *et al.* 2010a; Li *et al.* 2014). The full description of how the 48 double mutants were generated and validated and planted is provided in a previous study (Li *et al.* 2018). Briefly, the *Arabidopsis* plants were grown in two independent chambers with 16-hr light at 100–120 μEi light intensity with temperature set at a continuous 22°. The two growth chambers were set to identical abiotic environments but contain dramatically different biotic environments: one pest-free, with a clean Controlled Environment Facility (CEF) chamber as a typical laboratory growth condition; and one with an endogenous pest population, with a stress Life Sciences Addition building (LSA) chamber mimicking more natural growth condition. Seeds were imbibed in water at 4° for 3 days and sown into Sunshine Mix (Sun Gro Horticulture). Seedlings were thinned to one plant per pot (6 cm × 5 cm) at 7 days after planting. The pots were in 36 cell flats and each flat was considered as a blocking unit. All four genotypes (wild type, two single mutants, and one double mutant) for a double mutant combination were grown together in a single flat along with genotypes for other double mutant combinations, such that there was only a single representative of each genotype within the flat. This was replicated across

eight flats with randomization within each flat to create eight replicates of each genotype for each comparison. This experiment was conducted independently in the clean CEF and stress LSA chamber to generate a minimum of 16 biological repeats in total per genotype. The total combination of all genotypes required 24 flats per growth chamber. All genotypes were independently randomized within a flat.

Flowering time and plant growth measurement

All the plants were checked daily, and the flowering time, the first day of flowering after planting, was recorded for each of the plants. Pictures of all the plants were taken every other day from day 9 to 27, when some of the early flowering lines in the stress LSA chamber started to flower. The circling area of the rosette of each plant in each growth condition was manually measured in ImageJ across the days. The total circling leaf area was used as an indicator of the plant size. The plant flowering time and plant sizes were normalized relative to Col-0, and further visualized using the iheatmapr package in R software (R Development Core Team 2014).

Statistics

Each pair of TFs were separately analyzed using a repeated measures general linear model with lme4 to test for epistasis affecting plant growth (Bates *et al.* 2015). For this analysis each double mutant was tested using both single mutants and wild type grown concurrently with the following model: $y_{abc} = \mu + A_a + B_b + Ch_c + D_n + A_a \times B_b + A_a \times Ch_c + B_b \times Ch_c + A_a \times D_n + B_b \times D_n + Ch_c \times D_n + A_a \times B_b \times D_n + A_a \times Ch_c \times D_n + B_b \times Ch_c \times D_n + A_a \times B_b \times Ch_c \times D_n + P_i + \varepsilon_{abc}$, where P_i is the random variable of Plant, the experimental unit from which measurements were taken over time. ε_{abc}, the error term is assumed to be normally distributed with mean 0 and variance σ^2_{ε}. In this model, y_{abc} denotes the rosette area of each plant, genotype A represents the presence or absence of a T-DNA insert in one TF gene (wild type *vs.* mutant of locus A), and genotype *B* represents the presence or absence of a T-DNA insert in another TF gene (wild type *vs.* mutant of locus B) in the double mutant from chamber Ch_c (clean CEF chamber or stress LSA chamber). Time is represented by days, D_n. This model was run individually for each double mutant test and only the single mutants and wild-type Col-0 grown alongside the double mutants in the same flats were used in each model. This means that each double mutant test uses matched wild-type and single mutant control plants. Similarly, a general linear model was used to test epistasis affecting flowering time in each pair of TFs: $y_{abc} = \mu + A_a + B_b + Ch_c + A_a \times B_b + A_a \times Ch_c + B_b \times Ch_c + A_a \times B_b \times Ch_c + Ch_c{:}U_i + \varepsilon_{abc}$, where U_i is the random effect of blocks nested in chamber Ch_c. The ANOVA table, least-square means, and SE for each genotype by treatment combinations were obtained with lme4 and emmeans packages in R (Searle *et al.* 1980; Bates *et al.* 2015). The type III sums of squares from these models were used to calculate the variance and percent variance attributable to each term in the model. For the percent variance, this was calculated by comparing to the total variance in the model as the denominator. All network representations were generated using Cytoscape version 2.8.3 (Shannon *et al.* 2003).

To determine the power to identify significant epistatic and epistatic × conditional terms given our experimental design, we used the pwr.f2.test function from the pwr package (https://github.com/heliosdrm/pwr). Using the median number of error degrees of freedom across all models of 542 and a significance level of 0.05, we have a 0.8 power to detect significant epistatic and epistatic * conditional terms if the terms effect size (f2) is 0.0145 or higher. This is within the range of effect sizes linked to the epistatic or epistatic × conditional terms in our models (Supplemental Material, Figure S1). This indicates that we had sufficient power to identify epistatic × conditional using this experimental design (Figure S1).

In these analyses, we considered the 20 models for main effects or 48 models for the different epistatic comparisons as our independent tests. Using a nominal *P* value across 48 tests would suggest between two and three potential false positives per trait for the epistatic analyses. However, there was on average 20 (±2 SE) tests below 0.05 for the main epistatic interactions per trait and on average 8 (±1 SE) tests below 0.05 for the chamber × epistasis terms. This is much higher than the two or three expected false positives. To maximize our ability to compare across traits and genes, we have opted to utilize the less conservative nominal *P* values for the comparisons. Further, all *P* values and least-square means are reported to allow for direct assessment of the results (Tables S1 and S2).

Calculation of epistasis value

To study the effect of epistasis, we use epistasis value to describe the direction and strength of the epistasis. The epistasis value was calculated by normalizing the difference of observed double mutant phenotype *vs.* the predicted double mutant phenotype, assuming additivity of the single mutants, then normalized to the wild type as reported before (Segrè *et al.* 2005; Li *et al.* 2018). The phenotype for wild type was set as w, mutant TFa as a, mutant TFb as b, and double mutant TFa/TFb as ab. The epistasis value is calculated as {ab – [w + (a−w) + (b−w)]/w}. If the epistasis value is positive, this shows evidence for synergistic epistasis, while antagonistic epistasis is reflected in negative values. Larger the epistasis value signifies stronger the epistasis effects. The epistasis value were further visualized using the iheatmapr package in R software (R Development Core Team 2014).

Data availability

All genotypes are available upon request. File S1 contains all supplemental figures and tables mentioned within the text. Supplemental material available at figshare: https://doi.org/10.25386/genetics.11388195.

Results

Conditional growth effects of the 20 TF mutations

The 20 selected TFs were originally identified as binding aliphatic GLS-related promoters and their mutants influence

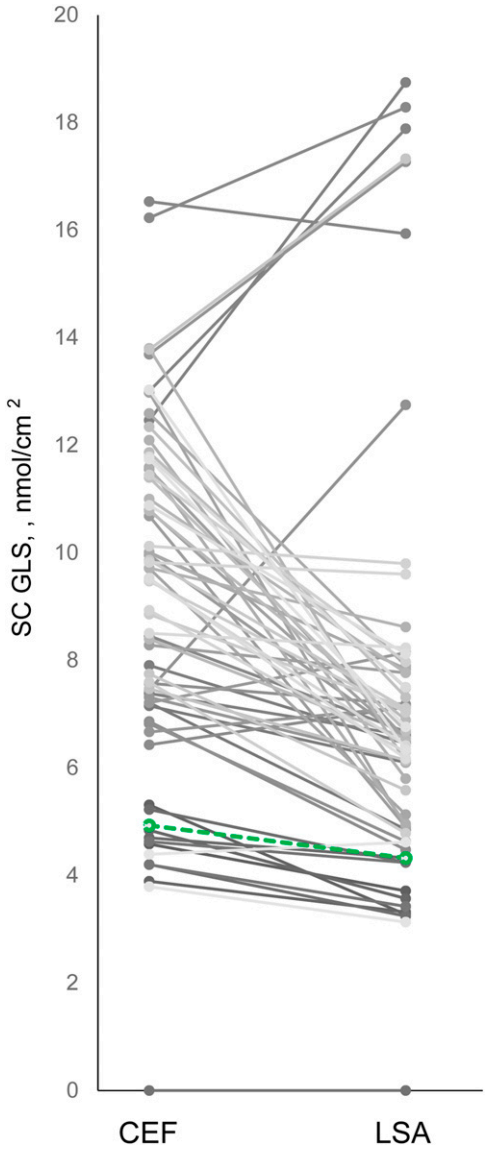

Figure 1 Extensive range of variation in short-chain GLS content of wild type, single mutants, and double mutants in CEF and LSA. The average absolute SC GLS content across all the genotypes in each growth chamber is shown. Wild type (Col-0) is highlighted as a green dashed line, while all the other genotypes are shown as gray solid lines.

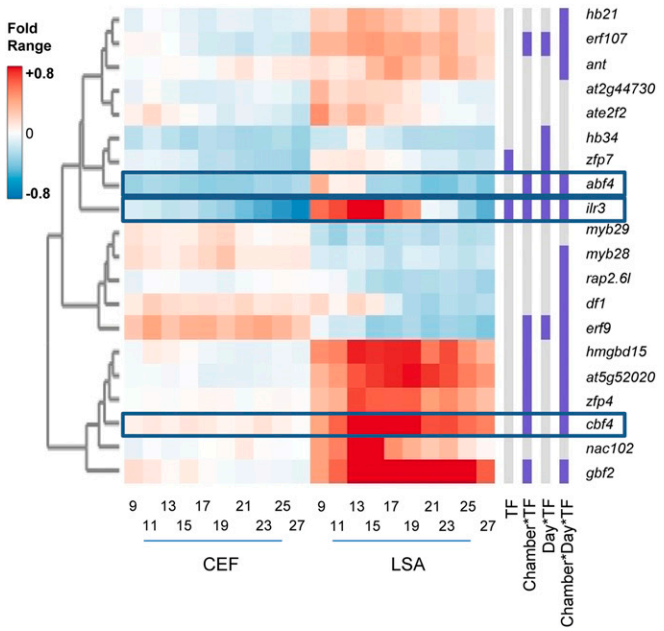

Figure 2 The effects of the 20 TFs on plant growth. The heatmap displays the fold change of plant size in single mutants, from day 9 to 27, in both the clean CEF chamber and stress LSA chamber. Red shows increased plant size and blue decreased plant size in comparison to Col-0. The columns on the right display the statistical significance (purple, significant $P < 0.05$; gray, not significant) for each term in the statistical model as listed at the bottom using the repeated measure model. Specific framed genotypes have mean phenotypes shown for reference in Figure S2.

aliphatic GLS accumulation (Li *et al.* 2014, 2018). We focused on the aliphatic GLS as they represent ~90% of the total GLS content within *Arabidopsis* leaves and therefore the majority of the metabolic flux. To measure the plant size in this mutant collection, we utilized digital image analysis on plants from two chambers, coded by their location in the CEF (clean chamber) and LSA (stress chamber) (Li *et al.* 2018). The two chambers, both built by Conviron, are similar in size, with identical light and humidity settings. The two chambers differ in their pest population: the clean CEF chamber is sterilized monthly after each planting while the stress LSA chamber contains longer-lived plants that maintain endogenous populations of pests likes fungus gnats, various flea beetles, aphids, *etc*. This creates a chamber that presents the plant with a blend of biotic pressures. Further, we acknowledge potential differences in the abiotic environments due to variation in ventilation or other parameters that were not controllable. Additionally, the mutant collection provides a large range of perturbation in defense chemistry independently of the different chambers that is similar to or even larger than the range of GLS variation in natural accessions (Figure 1) (Kliebenstein *et al.* 2001; Chan *et al.* 2010). This mutant collection generates a wider range of SC GLS defense variation than observed in multiple years of field trials for Col-0 (Kerwin *et al.* 2015). Thus, the LSA and CEF chambers test how the growth and defense in the mutant collection may or may not be sensitive to complex environmental perturbations (Figure 1).

Growth was measured every other day from 9 days post-germination to 27 days, at which time the leaves were overlapping. Plants were organized in a randomized complete block design with eight measurements per genotype per chamber (Li *et al.* 2018). The plant growth measurement spans the majority of vegetative growth providing a dynamic analysis of growth. Combining the data with repeated measure linear models, we tested for significant effects of all single gene TF mutants on growth across the conditions (Figure 2, Figure S2, and Supplemental Data Sets 1 and 2).

The models indicated that the influence of these TFs on growth is highly conditional on both plant age and growth chamber (Figure 2 and Figure S3). Of the 20 aliphatic GLS TF

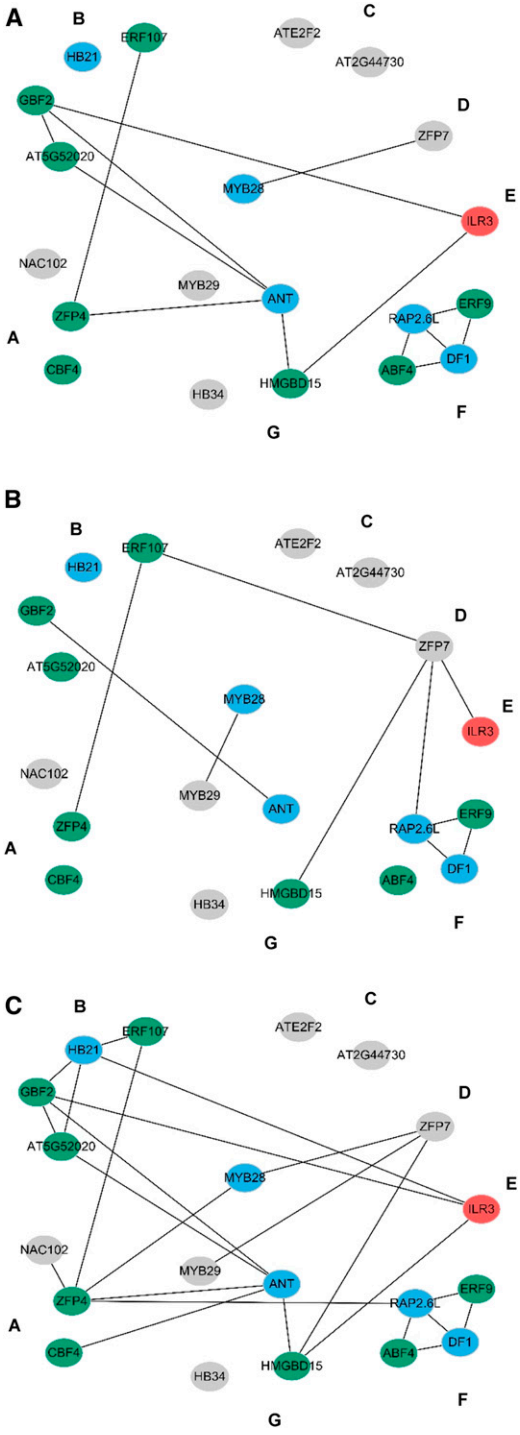

Figure 3 Epistatic interactions between TF genes modeled for plant growth. Epistatic networks for (A) TF × TF × chamber, (B) TF × TF × day, and (C) TF × TF × chamber × day. A line connecting two TFs correspond to a significant epistatic interaction. Node color indicates individual TFs' significance. Sky blue means that the individual TF has a significant genotype × chamber × day term, green means significant in both genotype × chamber × day and genotype × chamber terms, while red means significant in genotype × chamber × day, genotype × chamber, and genotype terms. Gray means not significant. (A–C) To maximize comparison across publications, the TFs are laid out in the network as groups A–G based on their modular effect on aliphatic GLS accumulation (Li *et al.* 2018).

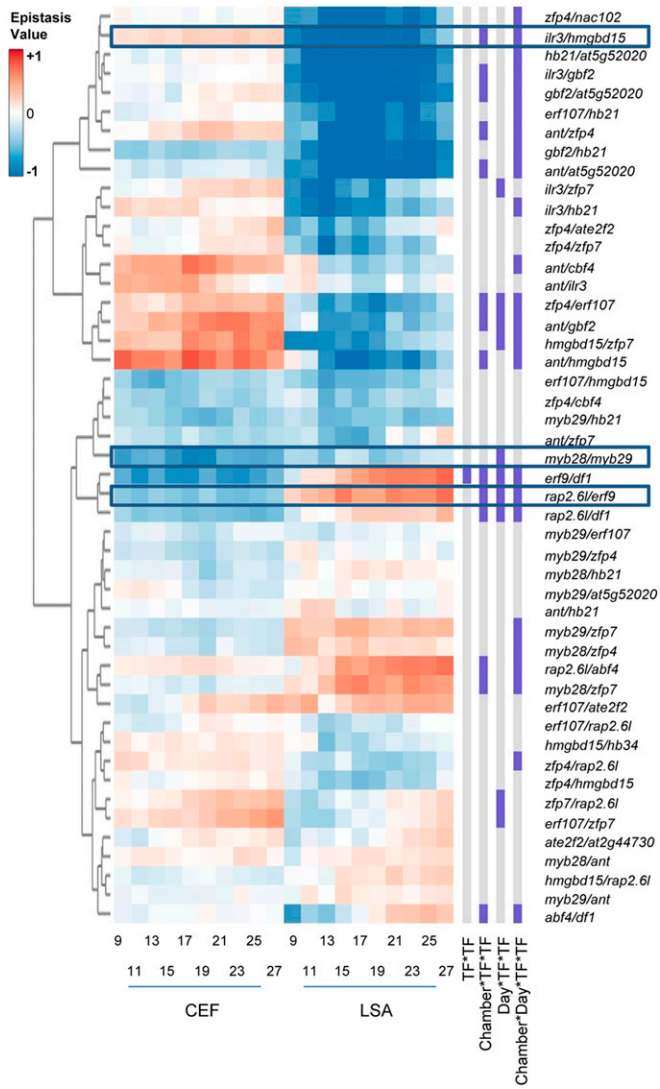

Figure 4 Epistatic effects on plant growth. Heatmap of epistasis values for all pairwise TF combinations from day 9 to 27 in each treatment condition. The genotypes are clustered using hierarchical clustering. The columns to the right of the heatmap show epistatic interaction terms as significant (purple) or not significant (gray) ($P < 0.05$). Framed genotypes are plotted in Figure 5.

mutants, 16 had a significant influence on growth. Strong positive growth effects were observed more often in the stress LSA chamber than in the clean CEF chamber for a number of TFs, like *HMGBD15*, *AT5G52020*, *ZFP4*, *CBF4*, *NAC102*, and *GBF2* (Figure 2). In contrast, *ABF4* had strong negative growth effects in both chambers. In addition to differences between the growth chambers, most of the TFs had differential influence across plant age. Some mutants combined these conditionalities as illustrated by *ilr3*, which had a transition at 21 days postgermination from positive to negative growth effects, but only in the LSA chambers (Figure S3). This conditionality illustrates the importance of large-scale phenotyping across different conditions to generate a broad view of how mutational effects may change dynamically (Figures S2 and S3). In an energetic trade-off, we would expect that most

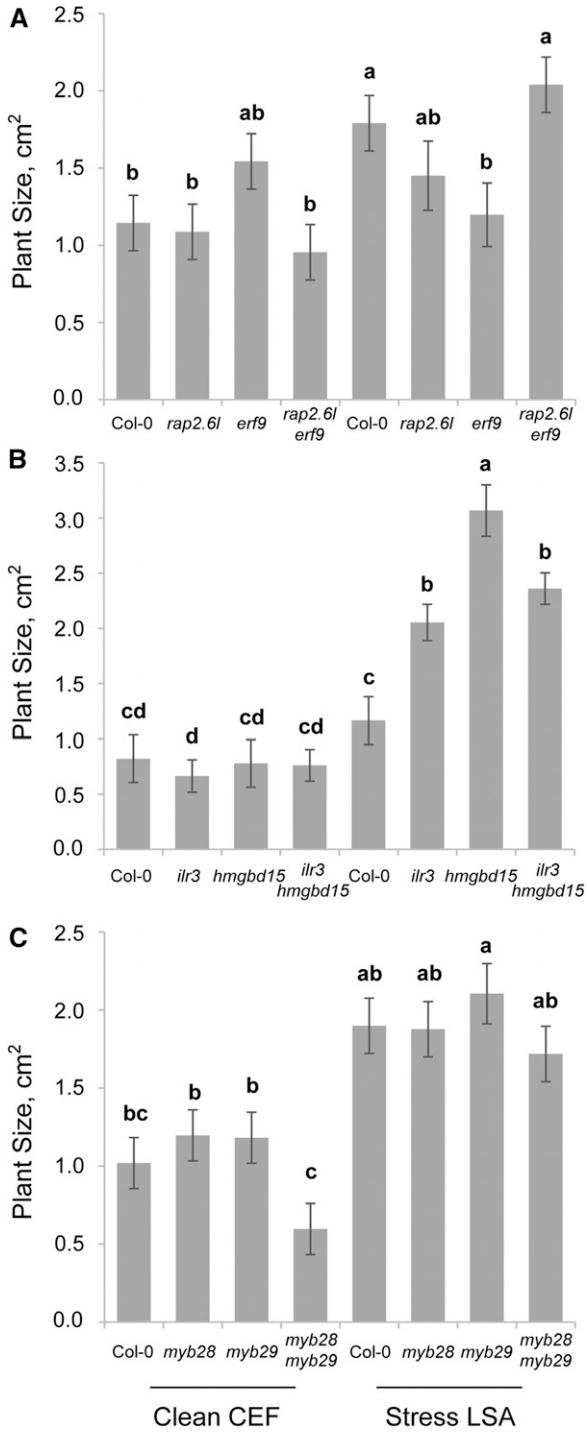

Figure 5 Epistatic growth phenotypes at day 15. The average rosette size on day 15 for three pairs of TFs in the clean (CEF) and stress (LSA) chambers. Each TF's pairwise combination has a wild-type (Col-0) genotype. Letters indicate genotypes with significantly different plant sizes. ($P < 0.05$ using *post hoc* Tukey's test). SE was calculated for eight samples per genotype and treatment. Day 15 was chosen to provide a common date across which to illustrate key differences. (A) Rosette size of single and double mutants of *rap2.6l* and *erf9*. (B) Rosette size single and double mutants of *ilr3* and *hmgbd15*. (C) Rosette size single and double mutants of *myb28* and *myb29*.

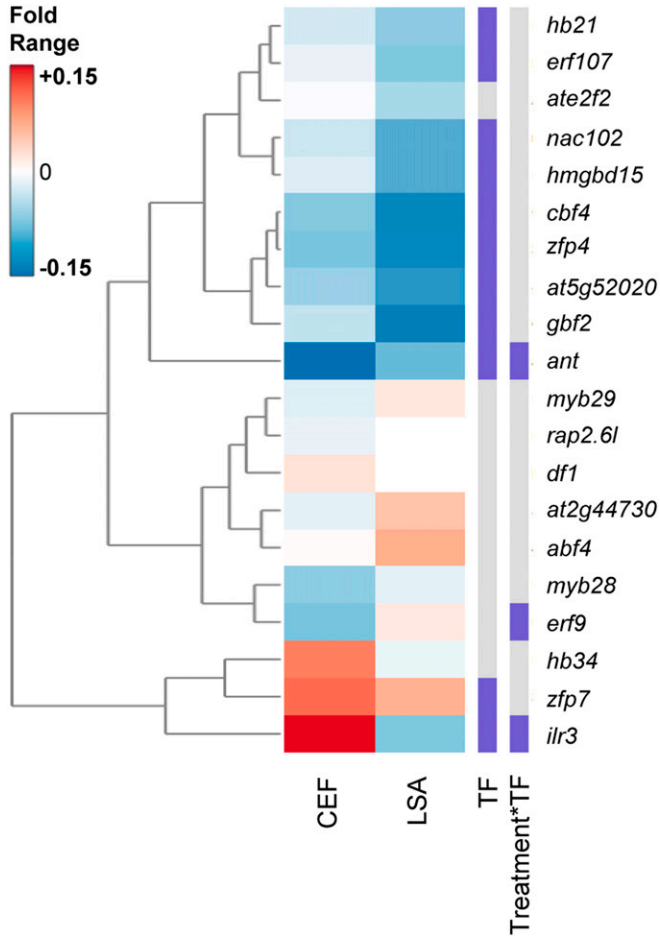

Figure 6 TF effects on flowering time. The heatmap displays the fold change of flowering time in the single mutants in both clean CEF chamber and stress LSA chamber. Red shows increased flowering time and blue decreased flowering time in comparison to Col-0. The columns on the right display the statistical significance (purple, significant $P < 0.05$; gray, not significant) for each term in the statistical model as listed at the bottom.

of these TF mutations should lead to smaller plants as these mutations increase aliphatic GLS content (Li *et al.* 2014). In contrast, the mutants had a mix of positive and negative growth effects. In addition, three mutants with strong aliphatic GLS phenotypes, *ant*, *myb28*, and *myb29*, have little to no detectable main effect on growth. One proposed alternative explanation for the *myb28* and *myb29* mutant is that these mutations often have a twofold increase in indolic GLS accumulation that may balance the loss in aliphatic GLS. However, because aliphatic GLS represent ~90% of the total GLS production, the GLS flux is still reduced by 80% in these mutants. The links between plant growth and defense via the aliphatic GLS in this TF collection supports the coordination model of growth and defense.

Dynamic epistatic networks underlying plant growth

We previously generated a set of 48 pairwise mutant combinations from 20 TFs controlling aliphatic GLS that form an

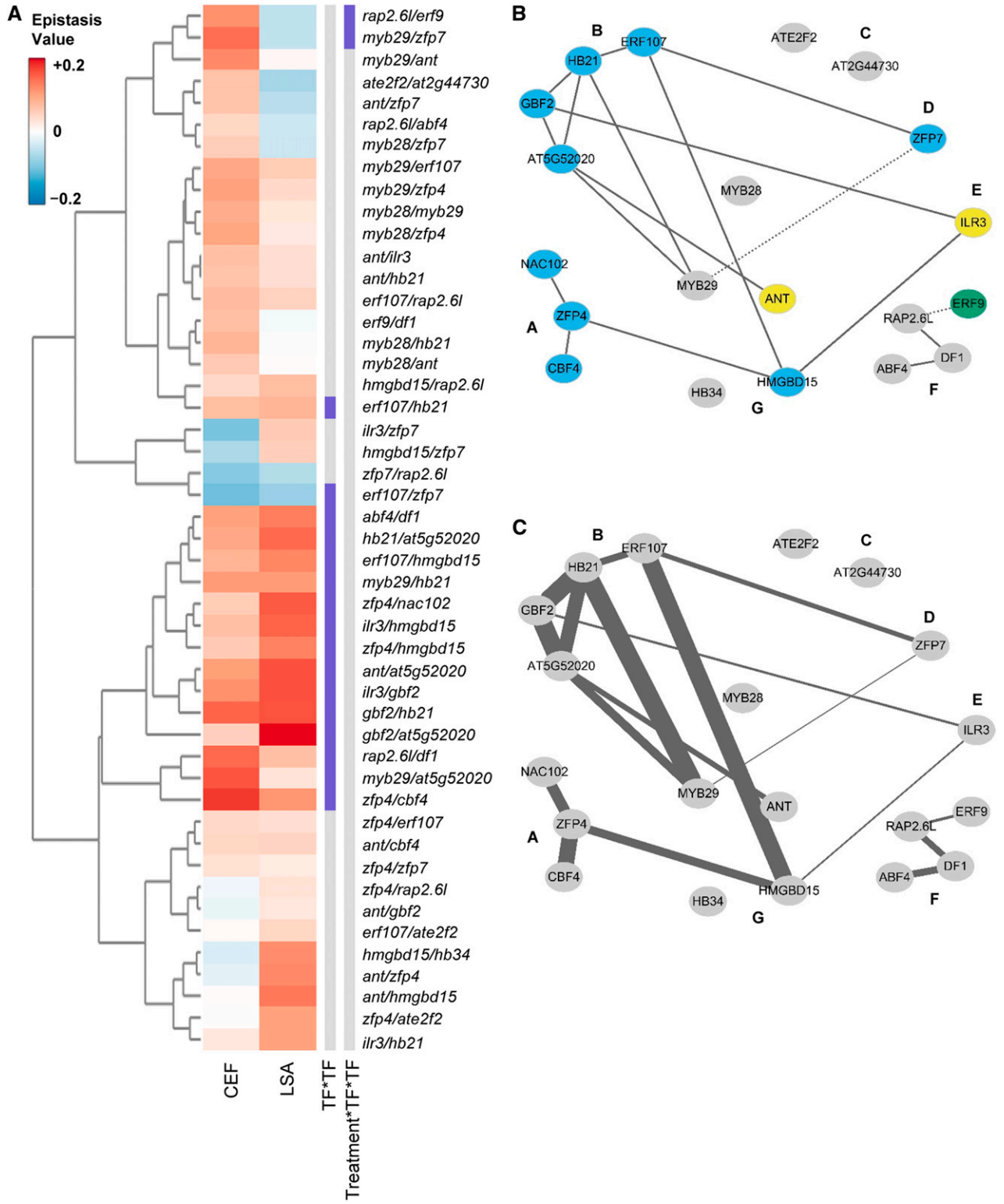

Figure 7 Epistatic network and flowering time effects. (A) Heatmap of epistasis values for all pairwise combinations individually in both treatment conditions. The genotypes are clustered using hierarchical clustering. The columns to the right display interactions as significant (purple) or not significant (gray) ($P < 0.05$). To maximize comparison across publications, the TFs are laid out in the network as groups A–G based on their modular effect on aliphatic GLS accumulation (Li *et al.* 2018). (B) A representation of the significant epistatic networks for flowering time. Solid lines indicate significant TF × TF interaction. Dotted lines indicate significant treatment × TF × TF interaction. Node color indicates individual TFs significance: sky blue, TF; green, treatment × TF; yellow, TF + treatment × TF; gray, not significant. (C) Visualization of individual epistatic variance components within the genetic network for flowering time. The width of the line connecting two TFs is proportional to the variance linked with the TF × TF term for that specific interaction.

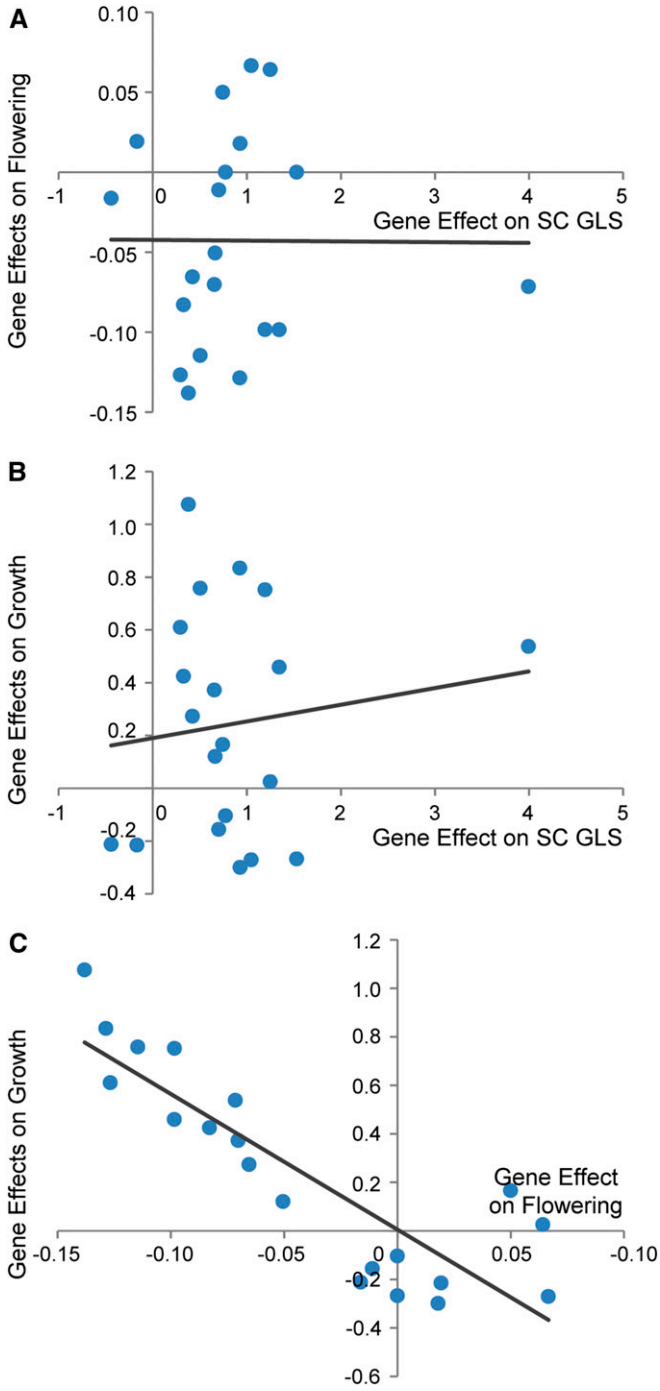

Figure 8 Lack of relationship between mutant effects on defense and growth. The main additive effect of the TF mutants in stress LSA chamber were selected to illustrate the absence of a relationship between growth, flowering time, and SC GLS. The predicted linear trend line and the statistical test results are shown. The axis shows the fold effect of the average mutant phenotype in comparison to the respective wild-type value. (A) Comparison of average gene effects on SC GLS and flowering time ($r = -0.006$, $P = 0.980$). This result was nonsignificant in both the presence and absence of the outlier point for SC GLS. (B) Comparison of average gene effects on SC GLS and growth ($r = 0.131$, $P = 0.583$). This result was nonsignificant in both the presence and absence of the outlier point for SC GLS. (C) Comparison of average gene effects on flowering time and growth ($r = -0.867$, $P < 0.001$).

extensive antagonistic epistatic network (Sønderby *et al.* 2007; Li *et al.* 2018). As these TFs affect growth individually, we used repeated measures linear models to assess if the epistatic effects were as prevalent on growth as on aliphatic GLS accumulation. We plotted the potential epistatic effects for each mutant pair and represented these interactions as a connectivity plot based on the mutants' main effects on aliphatic GLS (Figure 3, Figure 4, and Supplemental Data Set 3 and, 4). This analysis identified extensive epistatic interactions influencing growth. As observed in the single mutants, the epistatic interactions were equally conditional across ontogeny and growth condition (Figure 3 and Figure 4). These epistatic interactions followed a similar clustering as that observed when using GSL phenotypes for clustering. Particularly, the TFs in group F, *ERF9*, *DF1*, *ABF4*, and *Rap2.6L*, showed frequent epistatic interactions with each other for growth. Thus, this set of TFs identifies and illustrates an epistatic system that influences plant growth depending on age and growth condition. The effects of these TFs on growth are more conditional than the aliphatic GLS, suggesting that while the traits of growth and defense are both controlled by the epistatic network, they are independent regulatory outputs.

Conditional epistatic networks underlie plant growth

To quantify the epistatic effects on plant growth, we used a previously established epistasis value to measure the direction and magnitude of each epistatic interaction (Li *et al.* 2018). Briefly, we subtracted the measured double mutant phenotype from the predicted double mutant phenotype under an additive model. This value was then normalized to the wild-type phenotype. This epistasis value was measured for each pair of mutants for all the growth data (Supplemental Data Set 5). The epistasis value will be positive when there is synergistic epistasis and negative for antagonistic epistasis (Figure 4). Previous work showed that epistasis for SC GLS, the dominant form of aliphatic GLS, was almost entirely negative/antagonistic (Li *et al.* 2018). Unlike SC GLS, epistasis for growth was a mix of antagonistic and synergistic values that shift depending upon the conditions and developmental stages. For example, *rap2.6l* was involved in several epistatic interactions with other TFs from group F that were positive in the LSA growth condition but negative in the CEF growth condition (*i.e.*, *rap2.6/erf9*). In contrast, epistatic interactions involving *hmgbd15* had negative interactions in the LSA and positive interactions in the CEF growth conditions (*i.e.*, *ilr3/hmgbd15)* (Figure 4 and Figure 5). This argues that this epistatic network of TFs influences growth in both conditions, but that the environmental signals in the two conditions permeate differently through the TF network to generate variable growth outputs.

Epistatic networks influence flowering independent of tested environments

To test if these TFs and their network influence reproduction, we measured flowering time in all of the plants from all of the genotypes in the two contrasting chambers, and showed

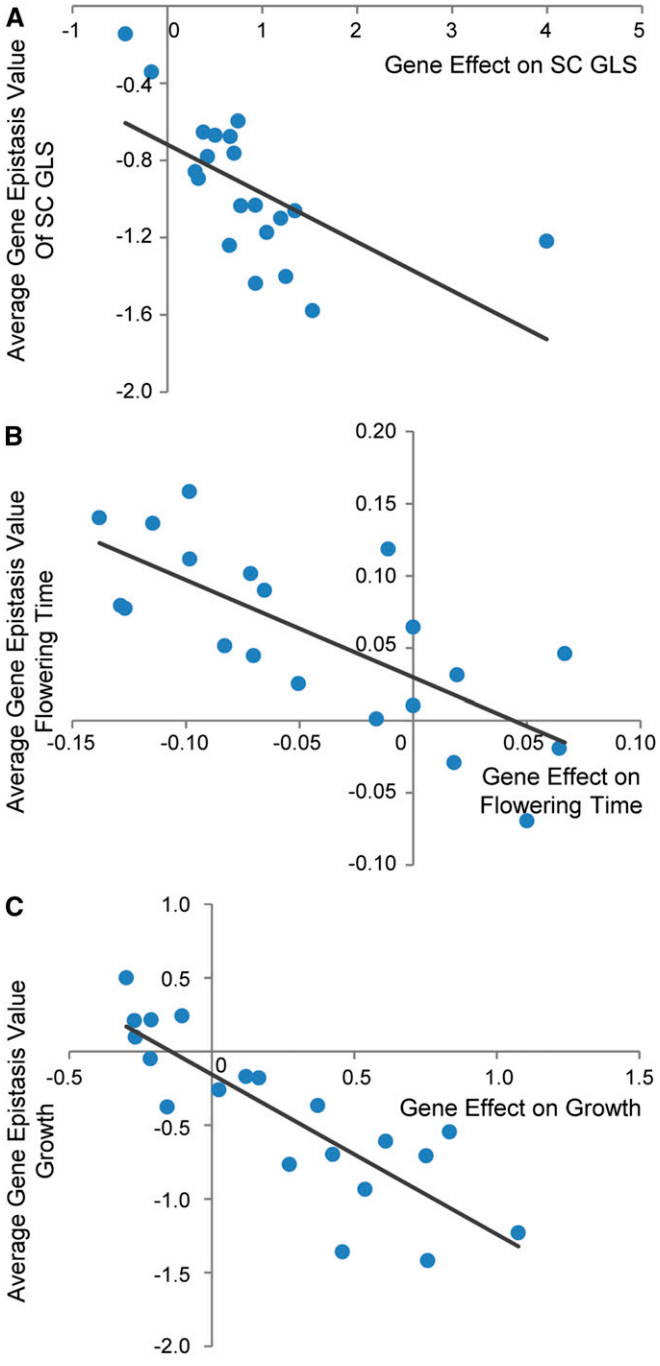

Figure 9 Relationship of the main and epistatic effects for TF genes. The average epistatic effect of a TF across all its pairs in the stress LSA chamber was calculated and compared to the TFs main effects for SC GLS, flowering time and plant size on day 17. The predicted linear trend line and the statistical test results are shown. The average epistasis value for each single gene across all its epistatic pairs is plotted against that gene's average single gene effect on the value as calculated against the respective wild type. (A) Comparison of average main gene and epistatic gene effects on SC GLS ($r = -0.610$, $P = 0.004$). This relationship was significant in both the presence and absence of the outlier point for SC GLS. (B) Comparison of average main gene and epistatic gene effects on flowering time ($r = -0.732$, $P < 0.001$). (C) Comparison of average main gene and epistatic gene effects on flowering time on growth ($r = -0.841$, $P < 0.001$).

that 12 of the 20 tested TFs significantly influenced flowering (Figure 6). However, unlike growth, the effects on flowering time were almost entirely toward early flowering in both chambers, with only *ANT*, *ILR3*, and *ERF9* having an environmental conditionality (Figure 6 and Figure S4). Plotting the epistatic effects for flowering time showed predominantly synergistic epistasis with 18 statistically significant interactions and only two interactions having environmental conditionality (Figure 7, A and B). This indicates that the genetic control of flowering time is less influenced by the environmental conditions than are either growth or aliphatic GLS. To further visualize how the epistatic variance was influenced by the network topology, we mapped the epistatic variance for the plant flowering (Figure 7C). Using previously ascribed groupings of the TFs based on their GLS phenotypes, TFs in groups A and B have more significant epistatic interactions partly overlapping with the epistatic interactions of growth phenotype, and TFs with strong main effects on flowering time also have higher genetic variance in their epistatic interactions.

Connections between defense and growth

To further explore the connection between plant defense and development, we systemically tested for associations between growth and defense in this data. These TFs predominantly influence the accumulation of SC GLS, and we used this as our quantification for defense (Supplemental Data Set 1) (Li *et al.* 2018). The mutant effects of the 20 TFs on SC GLS, plant growth and flowering time in both chambers were calculated by taking the phenotypic difference between mutant and wild type and normalized by the wild-type value. We then tested for a relationship between growth and defense by testing for correlations between the mutant effects using these traits (Figure 8 and Supplemental Data Set 6). In contrast to the expectation that an energetic trade-off model was solely driving this system, the TFs' effects on the accumulation of SC GLS and growth/flowering were largely uncorrelated (Figure 8, A and B). This was equally true in both the stress and clean chamber, indicating that stress did not illuminate a hidden relationship. As expected, there was a negative correlation between growth and flowering. Our findings show a highly complex relationship between plant defense and plant growth.

The connection of single mutant and double mutant effects

Given the low correlation between the SC GLS accumulation and plant growth, we proceeded to investigate if there may be any connection between a TF's main effect on a trait and its average epistatic effect on the trait. This allows us to investigate if there is any internal influence of single gene effects on the direction and value of their epistatic interactions. If there is a significant correlation, it would suggest that a gene's main effects can provide information about epistatic networks. To do this, we calculated each TF's average epistasis value for each trait across all the pairwise combinations involving that TF. Next, we correlated the TF's estimated single mutant effects

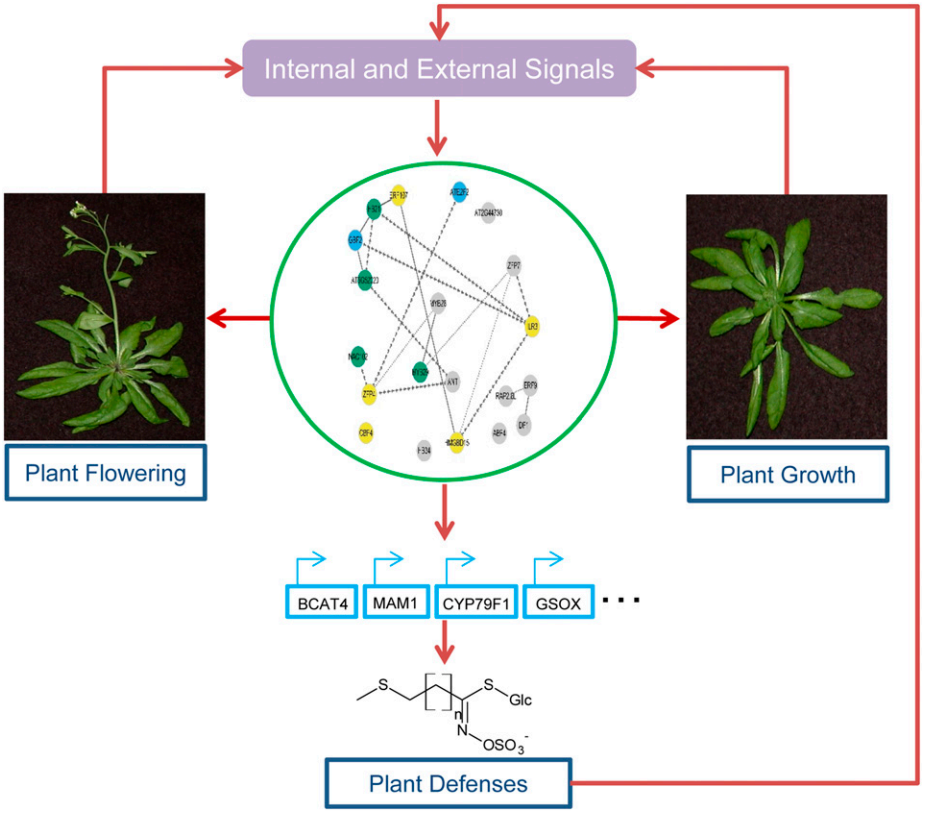

Figure 10 Proposed model for TF coordination of plant development and aliphatic GLS-based plant defense. External environmental and internal developmental signals are coordinately perceived via a group of TFs. Direct and indirect connections between these TFs allow for a coordinated response to these complex signals. A theoretically cohesive response is then transmitted to growth and defense via separate outputs from this network.

to their average epistasis value for each phenotype and chamber combinations (Figure 9 and Supplemental Data Set 6). The analysis showed that within all three tested traits, there are consistent negative correlations between a mutation's main and epistatic effects. One possible interpretation of this result is that the genetic background is constraining the results that we have obtained. There may be a maximal effect size within a background that would cause larger main effect TFs to invariantly have smaller epistatic interactions. The prevalence of negative epistasis in the SC GLS phenotype agrees with this possibility. Future work is required to understand if this observation is a general property of this network or is a function of the specific Col-0 accession in which it was conducted.

Discussion

In this study, we tested 20 TF mutants and 48 paired double mutants that influence aliphatic GLS accumulation to systemically explore whether these TFs also influence plant growth and flowering time. Seventeen of these 20 TFs significantly influence plant growth and flowering time. Interestingly, the key aliphatic GLS regulators *MYB28* and *MYB29* have little influence on plant growth and flowering. In addition, no simple mechanistic connection between the TFs' effects on the accumulation of aliphatic SC GLS, growth, or flowering was found. These findings fit with the emerging coordination model whereby a network is dynamic and highly responsive to the specific requirements of a specific environment. We propose that the internal and external signals are coordinated and perceived via connections between these diverse TFs. These connections create a decision matrix whereby growth and aliphatic GLS are interpreted and coordinated. Independent connections to growth and aliphatic GLS then proceed from this matrix to maximize plant fitness in a given environmental setting (Figure 10). Further, this suggests that TF networks provide an unappreciated potential to fine-tune both growth and defense to optimize modern agriculture.

Growth and defense vs. coordination

The canonical model for plant growth and plant defense is a trade-off model, which treats plant growth and defense as two competing biological processes under the assumption that the acquisition of elements and energy are limiting. As an alternative hypothesis, growth and defense are two separable outputs of the plant's regulatory system that must be coordinated depending on the specific environment. The analysis of the phenotypes in this TF collection and epistatic network in aliphatic GLS pathway supported the existence of the coordination model. The complex interactions between growth and defense depended on the specific perturbed TF, the environment and their epistatic effects. We found no consistent evidence of any negative relationship between the accumulation of the SC GLS defense metabolites and any measurement of growth. Future experiments will need to incorporate more complex regulatory relationships to truly understand how growth and defense are related in the field.

One complication to the interpretation of these results is pleiotropy associated with the use of T-DNA mutants. Recent work shows that individual *Arabidopsis* T-DNA mutants can have chromosomal rearrangements that could potentially affect the phenotype via off-target effects linked to growth pleiotropy (Jupe *et al.* 2019). However, those are likely limited to individual TFs and are unlikely to affect a whole collection of 20 TFs. We show that the whole collection supported a lack of a correlation between growth and defense. Further, recent evidence suggests that TFs that directly control GLS genes or GLS metabolites themselves can directly influence growth (Zhao *et al.* 2008; Kerwin *et al.* 2011; Khokon *et al.* 2011; Wang *et al.* 2011; Urbancsok *et al.* 2017; Zhu and Assmann 2017; Salehin *et al.* 2019). For example, MYB29 can control growth in response to differential nitrate potentially by its direct interaction with the *CCA1* promoter (Gaudinier *et al.* 2018). However, to fully understand how the plant is coordinating growth and defense will require a complete catalog of all TF-TF interactions at the protein and promoter levels. This catalog would clarify if genetic effects that we classify as indirect are in fact direct interactions that, instead of being a single molecular step, *i.e.*, TF to promoter, utilize a longer cascade of connected molecular processes than are typically studied.

Using transcription factors to tune and optimize growth and defense

Putative costs of plant defenses on growth have been intensively researched, and recent findings suggest that it is possible to promote one without sacrificing the other (Campos *et al.* 2016; Wang *et al.* 2018). Our current study further expands the future potential to optimize plant growth and defense through TF manipulation. Specifically, we found that a vast array of potential TFs can be identified and potentially used to manipulate plant growth and defense. In our system, mutations in more than half of the tested TFs could significantly promote plant growth and defense together across diverse environmental conditions. Critically, this ability to promote both defense and growth is conditional on specific environments. If this conditionality is true in other genes and TFs involved in plant growth and defense, it will raise the importance of studying plants' response to genetic manipulation under different growth conditions. This is particularly relevant to crop-breeding efforts in response to climate change and environmental stresses. However, studies involving larger collections of TFs and epistatic interactions across even more diverse environments are needed to further understand the coordination between growth and defense across fluctuating environments.

Acknowledgments

Funding for this work was provided by the National Science Foundation (awards IOS 1655810 and 1547796 to D.J.K.), the US Department of Agriculture National Institute of Food and Agriculture (Hatch project number CA-D-PLS-7033-H to D.J.K.) and by the Danish National Research Foundation (grant DNRF99 to D.J.K.). S.M.B. was partially funded by a Howard Hughes Medical Institute faculty scholar fellowship.

Literature Cited

Agrawal, A. A., 2011a Current trends in the evolutionary ecology of plant defence. Funct. Ecol. 25: 420–432. https://doi.org/10.1111/j.1365-2435.2010.01796.x

Agrawal, A. A., 2011b New synthesis-trade-offs in chemical ecology. J. Chem. Ecol. 37: 230–231. https://doi.org/10.1007/s10886-011-9930-7

Almeida-Cortez, J. S., B. Shipley, and J. T. Arnason, 1999 Do plant species with high relative growth rates have poorer chemical defences? Funct. Ecol. 13: 819–827. https://doi.org/10.1046/j.1365-2435.1999.00383.x

Alonso, J. M., A. N. Stepanova, T. J. Leisse, C. J. Kim, H. M. Chen *et al.*, 2003 Genome-wide insertional mutagenesis of *Arabidopsis thaliana*. Science 301: 653–657 (erratum: Science 301: 1849). https://doi.org/10.1126/science.1086391

Bates, D., M. Machler, B. M. Bolker, and S. C. Walker, 2015 Fitting linear mixed-effects models Using lme4. J. Stat. Softw. 67: 1–48. https://doi.org/10.18637/jss.v067.i01

Bekaert, M., P. P. Edger, C. M. Hudson, J. C. Pires, and G. C. Conant, 2012 Metabolic and evolutionary costs of herbivory defense: systems biology of glucosinolate synthesis. New Phytol. 196: 596–605. https://doi.org/10.1111/j.1469-8137.2012.04302.x

Beran, F., Y. Pauchet, G. Kunert, M. Reichelt, N. Wielsch *et al.*, 2014 Phyllotreta striolata flea beetles use host plant defense compounds to create their own glucosinolate-myrosinase system. Proc. Natl. Acad. Sci. USA 111: 7349–7354. https://doi.org/10.1073/pnas.1321781111

Bergelson, J., and C. B. Purrington, 1996 Surveying patterns in the cost of resistance in plants. Am. Nat. 148: 536–558. https://doi.org/10.1086/285938

Bidart-Bouzat, M. G., and D. J. Kliebenstein, 2008 Differential levels of insect herbivory in the field associated with genotypic variation in glucosinolates in *Arabidopsis thaliana*. J. Chem. Ecol. 34: 1026–1037. https://doi.org/10.1007/s10886-008-9498-z

Burow, M., B. A. Halkier, and D. J. Kliebenstein, 2010 Regulatory networks of glucosinolates shape *Arabidopsis thaliana* fitness. Curr. Opin. Plant Biol. 13: 348–353. https://doi.org/10.1016/j.pbi.2010.02.002

Campos, M. L., Y. Yoshida, I. T. Major, D. de Oliveira Ferreira, S. M. Weraduwage *et al.*, 2016 Rewiring of jasmonate and phytochrome B signalling uncouples plant growth-defense tradeoffs. Nat. Commun. 7: 12570. https://doi.org/10.1038/ncomms12570

Chan, E. K. F., H. C. Rowe, and D. J. Kliebenstein, 2010 Understanding the evolution of defense metabolites in *Arabidopsis thaliana* using genome-wide association mapping. Genetics 185: 991–1007. https://doi.org/10.1534/genetics.109.108522

Chan, E. K., H. C. Rowe, J. A. Corwin, B. Joseph, and D. J. Kliebenstein, 2011 Combining genome-wide association mapping and transcriptional networks to identify novel genes controlling glucosinolates in *Arabidopsis thaliana*. PLoS Biol. 9: e1001125. https://doi.org/10.1371/journal.pbio.1001125

de Lucas, M., L. Pu, G. Turco, A. Gaudinier, A. K. Morao *et al.*, 2016 Transcriptional regulation of Arabidopsis polycomb repressive complex 2 coordinates cell-type proliferation and differentiation. Plant Cell 28: 2616–2631. https://doi.org/10.1105/tpc.15.00744

Falk, K. L., J. Kastner, N. Bodenhausen, K. Schramm, C. Paetz *et al.*, 2014 The role of glucosinolates and the jasmonic acid pathway in resistance of Arabidopsis thaliana against molluscan herbivores. Mol. Ecol. 23: 1188–1203. https://doi.org/10.1111/mec.12610

Fan, M., M. Y. Bai, J. G. Kim, T. Wang, E. Oh *et al.*, 2014 The bHLH transcription factor HBI1 mediates the trade-off between growth and pathogen-associated molecular pattern-triggered

immunity in Arabidopsis. Plant Cell 26: 828–841. https://doi.org/10.1105/tpc.113.121111

Gaudinier, A., J. Rodriguez-Medina, L. Zhang, A. Olson, C. Liseron-Monfils *et al*., 2018 Transcriptional regulation of nitrogen-associated metabolism and growth. Nature 563: 259–264. https://doi.org/10.1038/s41586-018-0656-3

Guo, R., W. Shen, H. Qian, M. Zhang, L. Liu *et al*., 2013 Jasmonic acid and glucose synergistically modulate the accumulation of glucosinolates in Arabidopsis thaliana. J. Exp. Bot. 64: 5707–5719. https://doi.org/10.1093/jxb/ert348

Hemm, M. R., M. O. Ruegger, and C. Chapple, 2003 The Arabidopsis ref2 mutant is defective in the gene encoding CYP83A1 and shows both phenylpropanoid and glucosinolate phenotypes. Plant Cell 15: 179–194. https://doi.org/10.1105/tpc.006544

Huot, B., J. Yao, B. L. Montgomery, and S. Y. He, 2014 Growth-defense tradeoffs in plants: a balancing act to optimize fitness. Mol. Plant 7: 1267–1287. https://doi.org/10.1093/mp/ssu049

Jiao, Y., Y. Wang, D. Xue, J. Wang, M. Yan *et al*., 2010 Regulation of OsSPL14 by OsmiR156 defines ideal plant architecture in rice. Nat. Genet. 42: 541–544. https://doi.org/10.1038/ng.591

Joseph, B., J. A. Corwin, T. Zuest, B. Li, M. Iravani *et al*., 2013 Hierarchical nuclear and cytoplasmic genetic architectures for plant growth and defense within *Arabidopsis*. Plant Cell 25: 1929–1945. https://doi.org/10.1105/tpc.113.112615

Jupe, F., A. C. Rivkin, T. P. Michael, M. Zander, S. T. Motley *et al*., 2019 The complex architecture and epigenomic impact of plant T-DNA insertions. PLoS Genet. 15: e1007819. https://doi.org/10.1371/journal.pgen.1007819

Karban, R., and I. T. Baldwin, 1997 *Induced Responses to Herbivory*, University of Chicago Press, Chicago, IL. https://doi.org/10.7208/chicago/9780226424972.001.0001

Kerwin, R. E., J. M. Jiménez-Gómez, D. Fulop, S. L. Harmer, J. N. Maloof *et al*., 2011 Network quantitative trait loci mapping of circadian clock outputs identifies metabolic pathway-to-clock linkages in Arabidopsis. Plant Cell 23: 471–485. https://doi.org/10.1105/tpc.110.082065

Kerwin, R., J. Feusier, J. Corwin, M. Rubin, C. Lin *et al*., 2015 Natural genetic variation in Arabidopsis thaliana defense metabolism genes modulates field fitness. eLife 4: e05604. https://doi.org/10.7554/eLife.05604

Kerwin, R. E., J. Feusier, A. Muok, C. Lin, B. Larson *et al*., 2017 Epistasis x environment interactions among Arabidopsis thaliana glucosinolate genes impact complex traits and fitness in the field. New Phytol. 215: 1249–1263. https://doi.org/10.1111/nph.14646

Khokon, M. A., M. S. Jahan, T. Rahman, M. A. Hossain, D. Muroyama *et al*., 2011 Allyl isothiocyanate (AITC) induces stomatal closure in Arabidopsis. Plant Cell Environ. 34: 1900–1906. https://doi.org/10.1111/j.1365-3040.2011.02385.x

Kliebenstein, D. J., 2016 False idolatry of the mythical growth *vs.* immunity tradeoff in molecular systems plant pathology. Physiol. Mol. Plant Pathol. 95: 55–59. https://doi.org/10.1016/j.pmpp.2016.02.004

Kliebenstein, D. J., J. Kroymann, P. Brown, A. Figuth, D. Pedersen *et al*., 2001 Genetic control of natural variation in *Arabidopsis thaliana* glucosinolate accumulation. Plant Physiol. 126: 811–825. https://doi.org/10.1104/pp.126.2.811

Kliebenstein, D., D. Pedersen, B. Barker, and T. Mitchell-Olds, 2002a Comparative analysis of quantitative trait loci controlling glucosinolates, myrosinase and insect resistance in *Arabidopsis thaliana*. Genetics 161: 325–332.

Kliebenstein, D. J., A. Figuth, and T. Mitchell-Olds, 2002b Genetic architecture of plastic methyl jasmonate responses in Arabidopsis thaliana. Genetics 161: 1685–1696.

Koricheva, J., 2002 Meta-analysis of sources of variation in fitness costs of plant antiherbivore defenses. Ecology 83: 176–190. https://doi.org/10.1890/0012-9658(2002)083[0176:MAOSOV]2.0.CO;2

Kos, M., B. Houshyani, R. Wietsma, P. Kabouw, L. E. Vet *et al*., 2012 Effects of glucosinolates on a generalist and specialist leaf-chewing herbivore and an associated parasitoid. Phytochemistry 77: 162–170. https://doi.org/10.1016/j.phytochem.2012.01.005

Lambrix, V., M. Reichelt, T. Mitchell-Olds, D. J. Kliebenstein, and J. Gershenzon, 2001 The Arabidopsis epithiospecifier protein promotes the hydrolysis of glucosinolates to nitriles and influences *Trichoplusia ni* herbivory. Plant Cell 13: 2793–2807. https://doi.org/10.1105/tpc.010261

Li, B., A. Gaudinier, M. Tang, M. Taylor-Teeples, N. T. Nham *et al*., 2014 Promoter-based integration in plant defense regulation. Plant Physiol. 166: 1803–1820. https://doi.org/10.1104/pp.114.248716

Li, B., M. Tang, A. Nelson, H. Caligagan, X. Zhou *et al*., 2018 Network-guided discovery of extensive epistasis between transcription factors involved in aliphatic glucosinolate biosynthesis. Plant Cell 30: 178–195. https://doi.org/10.1105/tpc.17.00805

Lozano-Duran, R., A. P. Macho, F. Boutrot, C. Segonzac, I. E. Somssich *et al*., 2013 The transcriptional regulator BZR1 mediates trade-off between plant innate immunity and growth. eLife 2: e00983. https://doi.org/10.7554/eLife.00983

Mikkelsen, M. D., B. L. Petersen, E. Glawischnig, A. B. Jensen, E. Andreasson *et al*., 2003 Modulation of CYP79 genes and glucosinolate profiles in Arabidopsis by defense signaling pathways. Plant Physiol. 131: 298–308. https://doi.org/10.1104/pp.011015

Pajerowska-Mukhtar, K. M., W. Wang, Y. Tada, N. Oka, C. L. Tucker *et al*., 2012 The HSF-like transcription factor TBF1 is a major molecular switch for plant growth-to-defense transition. Curr. Biol. 22: 103–112. https://doi.org/10.1016/j.cub.2011.12.015

Pangesti, N., M. Reichelt, J. E. van de Mortel, E. Kapsomenou, J. Gershenzon *et al*., 2016 Jasmonic acid and ethylene signaling pathways regulate glucosinolate levels in plants during rhizobacteria-induced systemic resistance against a leaf-chewing herbivore. J. Chem. Ecol. 42: 1212–1225. https://doi.org/10.1007/s10886-016-0787-7

Paul-Victor, C., T. Züst, M. Rees, D. J. Kliebenstein, and L. A. Turnbull, 2010 A new method for measuring relative growth rate can uncover the costs of defensive compounds in Arabidopsis thaliana. New Phytol. 187: 1102–1111. https://doi.org/10.1111/j.1469-8137.2010.03325.x

R Development Core Team, 2014 *R: A Language and Environment for Statistical Computing*, R Foundation for Statistical Computing, Vienna, Austria.

Salehin, M., B. Li, M. Tang, E. Katz, L. Song *et al*., 2019 Auxin-sensitive Aux/IAA proteins mediate drought tolerance in Arabidopsis by regulating glucosinolate levels. Nat. Commun. 10: 4021.

Schlaeppi, K., N. Bodenhausen, A. Buchala, F. Mauch, and P. Reymond, 2008 The glutathione-deficient mutant pad2–1 accumulates lower amounts of glucosinolates and is more susceptible to the insect herbivore Spodoptera littoralis. Plant J. 55: 774–786. https://doi.org/10.1111/j.1365-313X.2008.03545.x

Searle, S. R., F. M. Speed, and G. A. Milliken, 1980 Population marginal means in the linear model: an alternative to least squares means. Am. Stat. 34: 216–221.

Segrè, D., A. Deluna, G. M. Church, and R. Kishony, 2005 Modular epistasis in yeast metabolism. Nat. Genet. 37: 77–83. https://doi.org/10.1038/ng1489

Shannon, P., A. Markiel, O. Ozier, N. S. Baliga, J. T. Wang *et al*., 2003 Cytoscape: a software environment for integrated models of biomolecular interaction networks. Genome Res. 13: 2498–2504. https://doi.org/10.1101/gr.1239303

Singh, K., R. C. Foley, and L. Onate-Sanchez, 2002 Transcription factors in plant defense and stress responses. Curr. Opin. Plant Biol. 5: 430–436. https://doi.org/10.1016/S1369-5266(02)00289-3

Sønderby, I. E., B. G. Hansen, N. Bjarnholt, C. Ticconi, B. A. Halkier *et al*., 2007 A systems biology approach identifies a R2R3 MYB gene subfamily with distinct and overlapping functions in regulation of aliphatic glucosinolates. PLoS One 2: e1322. https://doi.org/10.1371/journal.pone.0001322

Sønderby, I. E., M. Burow, H. C. Rowe, D. J. Kliebenstein, and B. A. Halkier, 2010a A complex interplay of three R2R3 MYB transcription factors determines the profile of aliphatic glucosinolates in Arabidopsis. Plant Physiol. 153: 348–363. https://doi.org/10.1104/pp.109.149286

Sønderby, I. E., F. Geu-Flores, and B. A. Halkier, 2010b Biosynthesis of glucosinolates–gene discovery and beyond. Trends Plant Sci. 15: 283–290. https://doi.org/10.1016/j.tplants.2010.02.005

Sussman, M. R., R. M. Amasino, J. C. Young, P. J. Krysan, and S. Austin-Phillips, 2000 The Arabidopsis knockout facility at the University of Wisconsin-Madison. Plant Physiol. 124: 1465–1467. https://doi.org/10.1104/pp.124.4.1465

Urbancsok, J., A. M. Bones, and R. Kissen, 2017 Glucosinolate-derived isothiocyanates inhibit Arabidopsis growth and the potency depends on their side chain structure. Int. J. Mol. Sci. 18: 2372. https://doi.org/10.3390/ijms18112372

Wang, R. S., S. Pandey, S. Li, T. E. Gookin, Z. Zhao *et al.*, 2011 Common and unique elements of the ABA-regulated transcriptome of Arabidopsis guard cells. BMC Genomics 12: 216. https://doi.org/10.1186/1471-2164-12-216

Wang, J., L. Zhou, H. Shi, M. Chern, H. Yu *et al.*, 2018 A single transcription factor promotes both yield and immunity in rice. Science 361: 1026–1028. https://doi.org/10.1126/science.aat7675

Wentzell, A. M., and D. J. Kliebenstein, 2008 Genotype, age, tissue, and environment regulate the structural outcome of glucosinolate activation. Plant Physiol. 147: 415–428. https://doi.org/10.1104/pp.107.115279

Zalucki, M. P., J. M. Zalucki, L. E. Perkins, K. Schramm, D. G. Vassao *et al.*, 2017 A generalist herbivore copes with specialized plant defence: the effects of induction and feeding by helicoverpa armigera (Lepidoptera: noctuidae) larvae on intact Arabidopsis thaliana (Brassicales) plants. J. Chem. Ecol. 43: 608–616. https://doi.org/10.1007/s10886-017-0855-7

Zhao, Z., W. Zhang, B. A. Stanley, and S. M. Assmann, 2008 Functional proteomics of Arabidopsis thaliana guard cells uncovers new stomatal signaling pathways. Plant Cell 20: 3210–3226. https://doi.org/10.1105/tpc.108.063263

Zhu, M., and S. M. Assmann, 2017 Metabolic signatures in response to abscisic acid (ABA) treatment in Brassica napus guard cells revealed by metabolomics. Sci. Rep. 7: 12875. https://doi.org/10.1038/s41598-017-13166-w

Züst, T., and A. A. Agrawal, 2017 Trade-offs between plant growth and defense against insect herbivory: an emerging mechanistic synthesis. Annu. Rev. Plant Biol. 68: 513–534. https://doi.org/10.1146/annurev-arplant-042916-040856

Züst, T., B. Joseph, K. K. Shimizu, D. J. Kliebenstein, and L. A. Turnbull, 2011 Using knockout mutants to reveal the growth costs of defensive traits. Proc. Biol. Sci. 278: 2598–2603. https://doi.org/10.1098/rspb.2010.2475

Communicating editor: J. Birchler